



## TANTALUM-NIOBIUM INTERNATIONAL STUDY CENTER

### PRESIDENT'S LETTER

Dear friends and members of the T.I.C.,

Time passes quite fast and we are already approaching our Fiftieth General Assembly, scheduled to take place in Tallinn, Estonia on Monday October 19th, as part of the T.I.C. meeting extending from Sunday October 18th to Wednesday October 21st 2009.

Without doubt, the economic crisis is having a large impact on our businesses, however, there is no point in hiding ourselves, not showing our faces to our business partners, old ones or potential ones, or not sharing points of view and topics of interest to our business community. That is what will make the world go round and will improve the market. Therefore, I encourage all our members to take the opportunity of coming to Tallinn in October.

As part of the programme, there will be a plant tour kindly hosted by Silmet, to its Sillamäe facilities.

We would like to encourage our members to submit their abstracts for technical papers as soon as possible or to indicate speakers to be invited.

The preparations for the meeting are well underway under the coordination of our Secretary General, Emma Wickens, and the Executive Committee will be meeting at the end of April in Brussels to finalize the programme and the arrangements. I am confident it will be another very successful event.

Please reserve those dates in your agenda and I look forward to seeing you all in Tallinn in October.

José Isildo de Vargas  
President

### TALLINN, OCTOBER 2009

The Tantalum-Niobium International Study Center is pleased to announce that it will be holding its Fiftieth General Assembly meeting in Tallinn, Estonia, from October 18th to 21st 2009. Delegates will stay at the Swissôtel, where the technical sessions and social events will also be held. The technical presentations will cover a wide range of topics related to the tantalum and niobium industries, and will take place in two half-day sessions to allow delegates a little spare time.

The business and administration of the association will be carried out in the formal General Assembly on the morning of Monday October 19th, including election of applicants for membership and the appointment of the members of the Executive Committee.

A plant tour to the facility of AS Silmet, in Sillamäe, will



*View of Tallinn, photo by Toomas Volmer, courtesy of Tallinn City Tourist Office & Convention Bureau*

be organised on Wednesday October 21st. Sillamäe is approximately two hours away from Tallinn, by bus.

AS Silmet processes both tantalum and niobium and commercialises these elements in the form of oxides, metal ingots, metal chips or metal powder. Silmet also specializes in rare earth production. After the second World War, 'factory nr 7', as it was then named, processed uranium. Production of metals and rare earths started in the 1970s, and the activities related to uranium ceased in 1990. At that time, the factory was renamed 'Silmet'. The company was privatized in 1997 and currently employs around 550 people. It maintains close cooperation with local universities in Tartu and Tallinn and boasts the best analytical laboratory in the metallurgy field within the Baltic States. Very conscious of the environment, Silmet has developed processes to recycle its waste streams into by-products and now functions without discharging any hazardous waste into nature.

Social events comprise a welcome reception on the evening of Sunday October 18th, and a gala dinner on the evening of Monday October 19th. We are also preparing an exciting programme of sightseeing tours for those accompanying delegates.

An invitation will be sent to the nominated delegate of each member company around mid-July. Others who would like to attend should contact the T.I.C. as soon as possible.

### CONTENTS

President's Letter .....	1
Tallinn, October 2009 .....	1
A New Method for Quantification of Texture Uniformity of Plate .....	2
Member Company News.....	8
Working Group on Tantalum and Niobium Mining.....	8

## A NEW METHOD FOR QUANTIFICATION OF TEXTURE UNIFORMITY OF PLATE

This article was prepared from the paper by Peter Jepson of H.C. Starck Inc. and Robert Bailey of Tosoh SMD, presented at the meeting of the T.I.C. held in Shanghai, China, in October 2008.

### INTRODUCTION

Sputtering is a physical vapor deposition (PVD) process for applying thin films to a substrate.<sup>(1)</sup> A sputtering target, the source of the material to be deposited, in the form of a plate, is held parallel to the substrate to be coated (figure 1). Between them is argon, at a pressure of a few milli-torr. The argon is excited to form a plasma, and since the target is held at a negative potential, positive argon ions are accelerated towards it and impact it at high velocity. 'Atomic billiards' occur as a consequence, as shown for tantalum in figure 2, and atoms are ejected from the target and deposited on the substrate, building up the film, which is typically required to be in the range of 50 to 500 nm. The secondary electrons emitted from the target are 'captured' by the magnetic field created by the magnetron, and when they collide with argon atoms, ionize them and increase the density of the plasma. The huge increase in sputtering rate caused by the magnetron turns sputtering from a laboratory curiosity into an industrial process, but it concentrates the argon ion collisions within a ring-shaped area of the target, so that area sputters preferentially and wears a 'race-track' groove into the target. Sputtering is one of the most important and most common processes used in the electronics industry: today's laptop computers contain sputtered films in the logic circuitry, in the memories, and in the flat-panel display. Tantalum, a bcc metal, is widely used as a diffusion barrier under copper interconnects in integrated logic circuits<sup>(2,3)</sup>: it is applied by sputtering. This is the example which will be used to illustrate the whole of this paper. A used tantalum sputtering target is shown in figure 3.

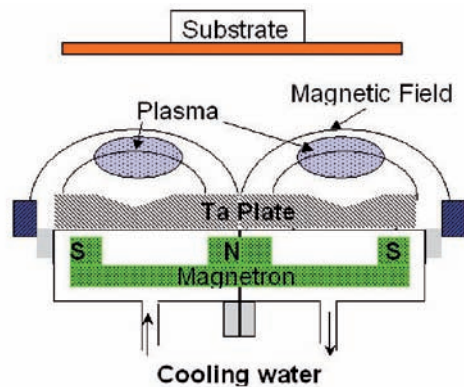


Figure 1: Sputtering equipment schematic

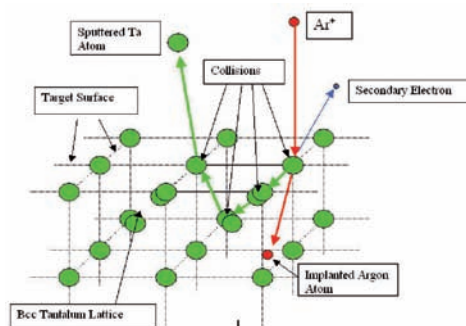


Figure 2: Atomic billiards



Figure 3: Used tantalum target

### UNIFORMITY OF THICKNESS

The uniformity of the film thickness is of major importance. Too thin a film at one point will not provide an adequate barrier, and too thick a film at another point will block a trench, or, if in an area from which it should be removed in a later step, will not be removed in the standard processing time. If the thickness of the film deposited is not within the range specified by the designer, the integrated circuit will not be fit for service, and the total cost of manufacture up to the point of test is lost, since no repair or rework is normally possible.

The uniformity of thickness of a film is assessed by measuring the thickness at many points, finding the standard deviation of the sample results, and expressing that as a percentage of the mean thickness. In the most stringent cases, uniformity of 2% is required. This performance level demands the most carefully-developed equipment and process parameters, but even in such a case, satisfactory results are only obtained from texture-controlled targets.<sup>(4)</sup>

### EFFECT OF GRAIN ORIENTATION ON SPUTTERING RATE

In sputtering, the orientation of a grain relative to the plate normal (ND) is most important. Orientation relative to directions within the plane of the plate is not so important, so 'grain orientation' as used in this paper refers to the orientation relative to ND. Various publications have discussed the effect of grain orientation on sputtering rate, with contradictory conclusions as to which orientations sputter fast and which sputter slowly. Zhang et al.<sup>(5)</sup> used a good experimental method, in which a target with very large grains was sputtered for a long time, after which the depth to which each grain had been eroded was measured. They found a ratio of sputtering rate of 2.1:1 between the fastest- and slowest-sputtering grains, but because none of the grains were very close to exact 100, 110 or 111 orientations, the ratio of the extremes may be greater.

The situation in the fine-grain material normally used for sputtering targets is complicated by the fact that grains of different orientation sputter at different rates thereby creating facets and steps at grain-boundaries.<sup>(6)</sup> Near the grain boundary the crystallographic plane of the surface is not the plane that the grain originally presented and, also, the impact of the argon ions is not normal to the surface.

Luckily, we do not need to worry about the sputtering rate of each individual grain or each individual facet, because 'averaging' occurs as the atoms cross the space from target to substrate: the atoms which make up the film at any given point (e.g. point A in figure 4) on the substrate come from many target grains. As a rule of thumb, the source of atoms for that given

point is a circle with a diameter half of the target-to-substrate spacing (area B), typically a circle of 10 cm diameter, which would contain over a million grains of 50  $\mu\text{m}$  size.

However, if area D has a texture (mix of grain orientations) different from area B, the film created at point C will be a different thickness from that created at point A. And of course, if the texture of one plate is different from that of another, the films formed from them will have different thicknesses.

It should also be mentioned that the directions in which atoms are sputtered are not random – rather, particular crystallographic directions are preferred.<sup>[7]</sup> However, when the sputtering process for a particular product is first developed, adjustments (primarily time of sputtering) can be made so the correct thickness is obtained. What is of greatest practical importance is the uniformity of texture, across the surface of the plate, through the thickness of the plate, and from plate to plate within each design.

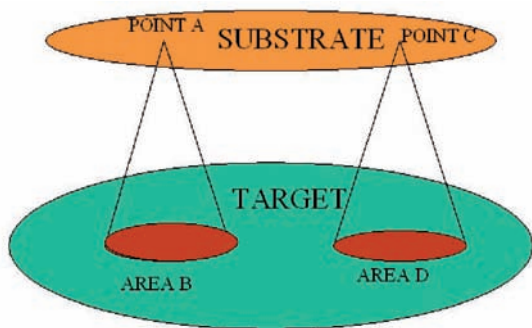


Figure 4: Target and substrate relationship

## TEXTURE OF TANTALUM PLATES

Most tantalum sputtering targets are manufactured from ingot, since vacuum-melting is a good refining method. Unfortunately, in the electron-beam drip melting system which is preferred in industry, the solidification is continuous from bottom to top, so an ingot consists of grains up to 1 m long, and several cm wide (figure 5). There is no practical way to control the orientations of those grains.

The traditional method of processing ingot to plate consists of side-forging and rolling (thereby reducing the ingot diameter, typically 200 mm, to the thickness of the plate, e.g. 8 mm), with perhaps one intermediate anneal and one final anneal. The texture of the resulting (once or twice recrystallized) material is banded, with the bands corresponding to the original ingot grains, as illustrated in figure 9. In some metals, when subjected to compressive strain in a single direction, the grains gradually all rotate to the same orientation, resulting in a texture which approaches uniformity as the strain is increased. In tantalum, however, depending on its initial orientation, a grain may rotate either towards  $[100] // \text{ND}$  or towards  $[111] // \text{ND}$ . Thus, figure 9 and subsequent maps are predominantly blue and red.

Given then that, on the one hand, a plate ideal for sputtering has uniform texture throughout its volume, and the same texture as every other plate, while, on the other, the traditional manufacturing methods result in plates with considerable non-uniformity within the volume, and variation from plate to plate, considerable effort has been invested by industry in the last ten years in developing thermo-mechanical processing methods that eliminate, or at least minimize, the texture non-uniformities.<sup>[8,9]</sup>

Even when the ingot is homogenized before rolling, there tends to be a texture variation from near-surface to mid-thickness of the

plate, caused by differences of the strain pattern during rolling. Figure 10 illustrates this through-thickness texture gradient, showing an example which does not have strong banding, though in practice the two effects may be superimposed.



Figure 5: Ingot longitudinal section

## MEASUREMENT OF TEXTURE

It is impossible to develop a manufacturing process unless there is a measurement of the success of the experimental lots, and sputtering through a plate and assessing the thickness of the films produced is so slow and expensive as to be impractical. Therefore texture is measured on plate samples by EBSD. The same type of texture measurement can also be used in production, as a method of Quality Control. A method which measures texture grain by grain is clearly called for in this situation.

Because of the aversion common in industry to destroying good product for the sake of characterizing it, samples are typically taken from near the edge of a rolled plate (figure 6). It is normal practice to prepare and examine a through-thickness section, even though a planar section (squares) could be more directly related to the sputtering performance, because more information can be gained from the former. The area examined by EBSD (diagonally-shaded area) includes the full thickness. The EBSD step used is nominally 1/3 the grain size (average linear intercept, or ALI). Since 45  $\mu\text{m}$  is a typical ALI, a 15  $\mu\text{m}$  step is often used. A smaller step would result in a truer (less pixellated) grain map, but would take longer. If a larger step were used, the chance of missing the smallest grains altogether would become a concern.

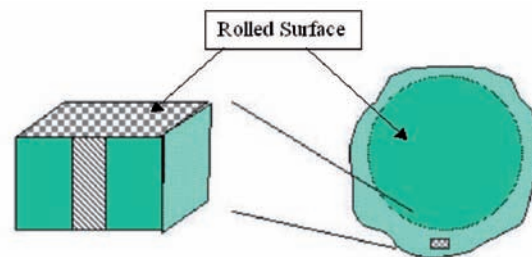


Figure 6: Typical sample location

Grain maps are typically displayed after rotating the diagonally-shaded area of figure 6 counter-clockwise by 90°. Thus, figure 9 has the rolled surfaces at left and right, and represents an area approximately 8 mm (the thickness of the plate) by 2 mm. The colours of the grains show their orientation relative to ND (which is now horizontal). Figure 7 shows the colour scheme commonly used for displays. The red (100), blue (111) and yellow (110) sectors extend 20° from the pole, with the colour becoming less bright as the misorientation increases. Figure 8 shows the colour scheme which illustrates the calculations to follow: here the colours are uniform, extending 15° from each pole, because a grain is counted as a 100 grain, for example,

if that grain has a [100] direction within 15° of ND. This colour scheme is the preferred one because it uses the three primary colours, which stand out equally, because it emphasises the misorientation of each grain from its nearest 'ideal' orientation, and because, having sharp cut-offs, it allows area percentages to be calculated.

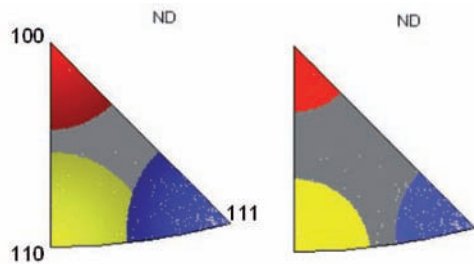


Figure 7: Colour scheme for display

Figure 8: Colour scheme for calculation

## QUANTIFICATION OF RESULTS

The grain maps are very useful in that they show the texture banding and the texture gradients, and they served well for some time for process development purposes. However, soon, questions like 'How severe is the banding?' and 'How would you decide whether one lot of plates was significantly different from previous lots?' demanded quantitative answers.

The first noteworthy attempt to quantify the non-uniformity of tantalum texture was made by Michaluk et al.<sup>(10)</sup> However, this method did not achieve wide acceptance in industry, for two reasons: because it was patented and no licenses were allowed, and because it used very complicated calculations, involving integration through the thickness of the first and second derivatives of the pole deviation function. A new effort to work out a method was initiated in 2005. Borrowing some of the concepts of the Michaluk method, it included input from most of the companies involved commercially in tantalum sputtering targets.

The new method quantifies three features of plate texture: the strengths of the components, the severity of banding of each component, and the gradient of each component. These features are measured independently of one another. The texture of the plate being nominally symmetrical about its mid-thickness centre-line, the texture of each half is analyzed separately.

The strengths of the components (100 // ND and 111 // ND are normally the two major components in tantalum plate) are measured as the area percentage of each half-thickness, using the 15° cut-off. For the sake of the example, let us examine figure 11, which is the 'top' half of figure 10. Of this area, 22% is red (100), 32% is blue (111) and 5% is yellow (110). Often the 110 component is ignored, if it is much smaller than the others. This measurement is preferred over the traditional 'times random' peak height because it does not depend on the operator's discretion in setting a calculation parameter (the half-width). Figure 12 illustrates the effect of two settings of half-width on the data set: the 'times random' maximum varies from 6.5 to 3.2. Also, the area percentage method results in only a small error if there is a slight (1° or 2°) experimental misalignment of the sample, which is a common occurrence.

**www.tanb.org**  
**e-mail to**  
**info@tanb.org**

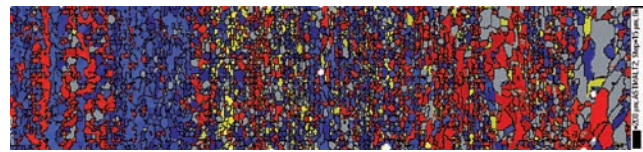


Figure 9: Plate with banded structure. Area approx. 8 mm x 2 mm, with rolled surfaces at left and right, and ND horizontal

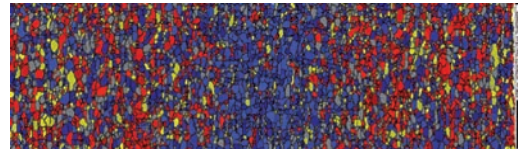


Figure 10: Plate with through-thickness gradient and slight banding (10 mm thick)

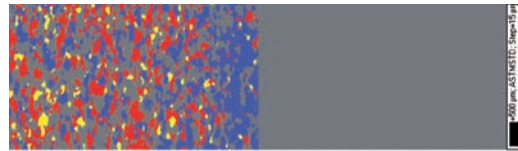


Figure 11: Top half of figure 10, in 'calculation' colours

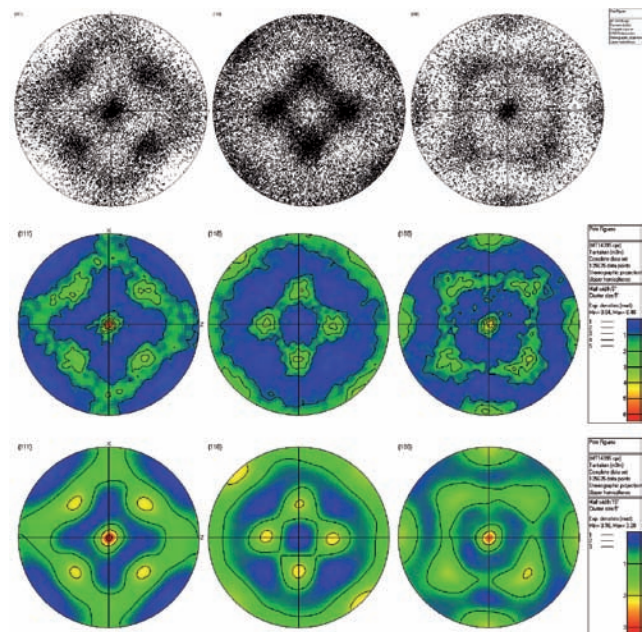


Figure 12: Pole figures with varying half-angles

Quantifying (independently) gradient and banding severity is not so simple. Various ideas were tried, and considered on the criteria of correspondence to visual impressions from grain maps and ease of calculation. The method chosen is based on the concept of a moving window originally proposed by J.A. Sutliff.<sup>(11)</sup> A window is a small part of the total area. The window must be small enough that it does not contain multiple bands, but not so small that 'noise' overpowers 'signal'. The optimum size for the window has been determined to be 60 grains (60 x ALI) parallel to the rolled surfaces, by 3 grains in the thickness direction.

First the window is set at one end of the examined area (i.e. at the surface) and the area percentages of the components of interest calculated. Then the window is moved one step away from the surface and the calculations repeated. This procedure is repeated until the window reaches mid-thickness. Figure 13 illustrates two of the many window positions as figure 11 is analyzed. In this way a graph such as figure 14 is created, the left side of which represents the near-surface material, and the right side the mid-thickness. Now the best-fit straight lines can be added, and their slope is a measure of the texture gradient

('s100' and 's111'), expressed as % per mm. Furthermore, the points not all being exactly on the best-fit line, the vertical distance between each point and the line can be measured, and the average of those distances is a measure of the severity of banding of each component ('B100' and 'B111'). It is expressed as %.

In figure 14 the blue dots in particular appear to approximate a curve, rather than a straight line, so the banding severity is over-estimated. In such a situation, a polynomial can be used as the base-line for banding severity calculation. Figure 15 shows the results if a fourth-order polynomial is fitted (with the constraint that it is horizontal at the right-hand side, which is the mid-thickness): B111 is reduced significantly (7.8 to 5.6%).

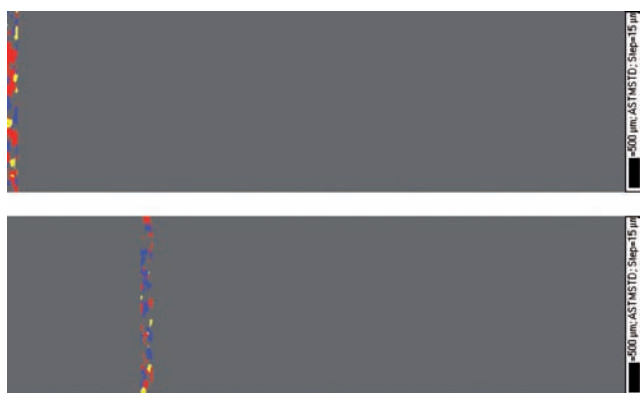


Figure 13: Two positions of the window moving across a half-thickness (same data set as figure 11)

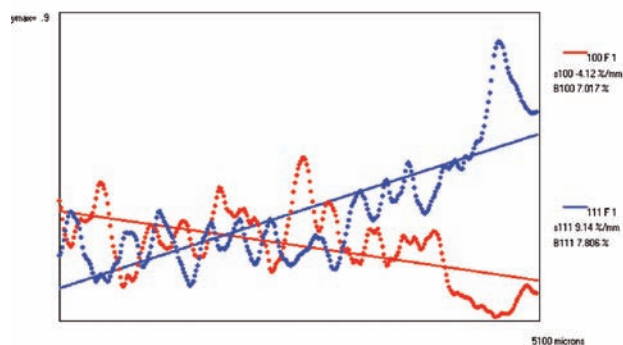


Figure 14: EBSD Grad plot of data set from figure 11 (straight line fit)

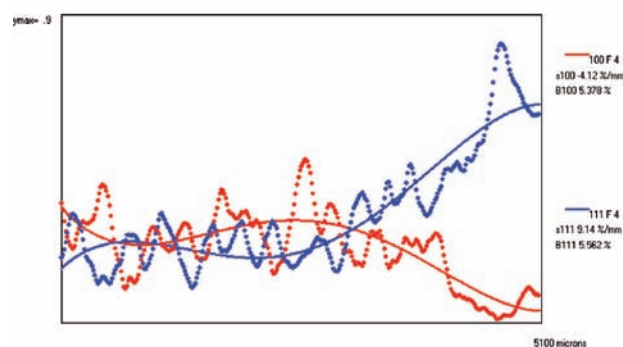


Figure 15: EBSD Grad plot of data set from figure 11 (fourth-order polynomial fit)

## EXACT METHODS OF CALCULATION

### Input data file

The input to the software analysis program is a data file generated by the EBSD analysis software. Information at each measurement point (pixel) in the EBSD sample is entered into the data file as an individual 'pixel record'. The following information in each pixel record is needed for the analysis described here:

- x-location of the pixel (in microns), representing distance through thickness
- y-location of the pixel (in microns), representing distance parallel to the rolled surface
- the Euler angles,  $\phi_1$ ,  $\Phi$  and  $\phi_2$ .<sup>(12)</sup>

The 'as-measured' orientation is relative to the surface normal of the cross-section sample. It is necessary to rotate this orientation (by 90°) so that it is relative to the original target surface normal (ND). This rotation can be performed by the original EBSD analysis program and saved to the data file 'already-rotated', or it may be saved in the as-measured state. In the latter case, the Gradient & Banding software<sup>(13)</sup> will need to perform the rotation. The angle  $\phi_1$  is only needed to make this rotation. Once rotated, only  $\Phi$  and  $\phi_2$  (the inverse pole figure angles) are used in the analysis.

### 'x-step' definition

The entire data set is broken into thin slices perpendicular to the x direction. The crystallographic texture is averaged (over the y direction) in each slice and saved in an array. The width of each slice is the x-step distance. It is specified as an integer multiple (n-step) of the minimum e-beam stepping increment in the x direction used to create the pixel map. Usually an n-step of 1 is used. If the particular data set is very large (small e-beam stepping distance), a larger n-step might be chosen in order to make cleaner looking plots.

### 'x-window' definition

The x-window is the width of a thicker slice (also perpendicular to the x direction) over which the crystallographic texture is averaged. It is defined as an integer multiple (n-window) of the x-step distance. Typically, n-window is picked to obtain an x-window value approximately three times the average grain size for the sample. The texture components are averaged within a band of this width, as the band is stepped along the x direction by the x-step distance.

### Data analysis - array filling

The first step is to reduce the two-dimensional pixel map data into a series of one-dimensional arrays. The length of these arrays, n-count, depends on the x-step distance:

$$'n - count' = \frac{'sample - thickness'}{'x - step'} + 1$$

A separate array is needed for each component of texture that is being analyzed plus an additional array for the total count. In this discussion we assume that only the following texture components are being analyzed: (100), (110) and (111). Four arrays (each of length n-count) are needed to receive the data from the input file, i.e. F100, F110, F111 and Ftotal. For each point in the pixel map, the x-location determines the index location for updating the arrays:

$$index = \frac{'x - location'}{'x - step'} + 1$$

The Euler angles  $\Phi$  and  $\phi_2$  determine the location of the target surface normal (Nt) within orientation space (i.e. inverse pole figure). These two angles, respectively, can range from 0 to 90°, and from 0 to 360°. For each pixel in the data file, it is necessary to calculate the angle of Nt with each orientation direction (including multiplicity directions) for the relevant texture components. For the three components (100, 110 and 111) there are 26 angles to calculate. By applying crystal symmetry operations, the ranges for  $\Phi$  and  $\phi_2$  can be reduced, decreasing the number of angles to calculate. The smallest angle found determines the texture component 'candidate' (either 100, 110 or 111). That angle is then compared to the 'cut-off' angle. If it is less than the 'cut-off' angle the candidate array is incremented (i.e.  $F100(\text{index})=F100(\text{index})+1$ ). The total-count array is incremented ( $Ftotal(\text{index})=Ftotal(\text{index})+1$ ).

After completing this for the entire data file, the volume fraction of each texture component has been calculated as a function of the depth direction (x) with a depth resolution of x-step. For example the volume fraction of (100) at a depth x is given by:

$$VF100 = \frac{F100(i)}{Ftotal(i)}, \text{ where } i = x / \text{'x-step'} + 1$$

Depending on the value of x-step and the width of the sample (ymax) the resulting arrays can be very 'noisy' due to a small sample size.

A second copy of each array is created which sums the data over a moving band of width n-window. For example:

$$C100(i) = \sum_{j=0}^{\text{'n-window'-1}} F100(i + j)$$

In this set of arrays, the number of data points has been reduced to 'c-count' = 'n-count' - 'n-window' + 1. These 'smoothed' arrays will be less noisy and are used for the gradient and banding analysis described below.

The original arrays can be saved to permit relatively quick calculation time using different x-window settings.

### Gradient Analysis

The 'smoothed' arrays are evaluated by fitting a straight line to the data (using linear regression). For Ta analysis we choose to evaluate the gradients for the (100) and (111) texture components. These gradients are typically reported in units of volume fraction % (equivalent to area %) per mm (%/mm). Since this gradient analysis is typically only applicable to half thickness samples, it is important to crop the original EBSD pixel maps to the correct locations. Alternately the analysis program can allow the user to select the appropriate area of the map to calculate the gradient calculation.

### Banding Analysis

The 'smoothed' arrays are evaluated by fitting a polynomial to the data. The average deviation of the data to the polynomial (absolute value of the difference) is used as the banding severity number. It is reported in volume fraction %. Usually a polynomial of order 4 or less is used.

## COMPARISON OF VISUAL IMPRESSION TO CALCULATION RESULTS

The results of figure 14, compared to the appearance of figure 10 (left-half), can be used as a baseline. Let us compare the plate shown in figure 9 to that of figure 10. Figure 16 shows the left-half of figure 9 (as part of the EBSD Grad software

working screen), and figure 17 is the resulting plot. Higher banding severities (12.8% for 100, 20.4% for 111) are seen in figure 17 than are seen in figure 14 (7.0 and 7.8%), as expected from the (severely-banded) appearance of figure 9. The gradients are not very meaningful in this case, since banding dominates the non-uniformity.

On the other hand, figure 18 shows a plate with no discernible banding, and only a slight gradient. The gradients calculated by EBSD Grad for the left-half of the data set and seen in figure 20 (3.3 and 6.3) are lower than those of figure 14 (4.1 and 9.1), as expected. When a data set with, in reality, no banding, is analyzed, the calculated banding severity is not zero, because of 'noise' (the numbers in a random data set are not evenly distributed): it is about 4%, and figure 20 shows banding of this order for this example. This noise level can be reduced by increasing the width of the area examined, but excess width could result in a band being missed if it is not exactly parallel to the surface, as often occurs, so a compromise must be made. Note that figures 14, 17 and 20 have different scales on the y-axis (and that figures 16 and 19 are upside-down compared to figures 9 and 18).

Many more examples could be shown, but for all of them, there would be correspondence between visual impression and calculation results, except for the addition of about 4% 'noise' to the banding severity.

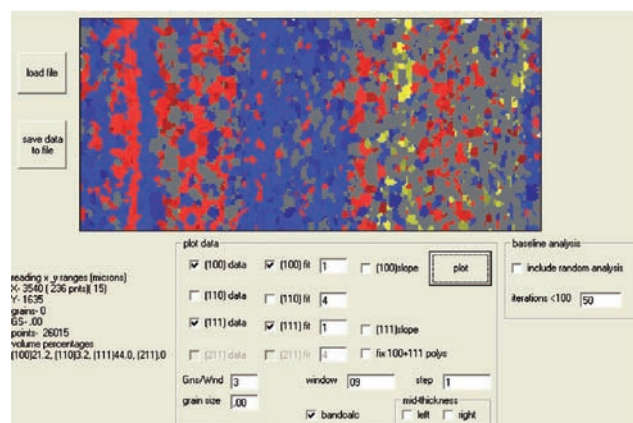


Figure 16: EBSD Grad working screen, data set from figure 9

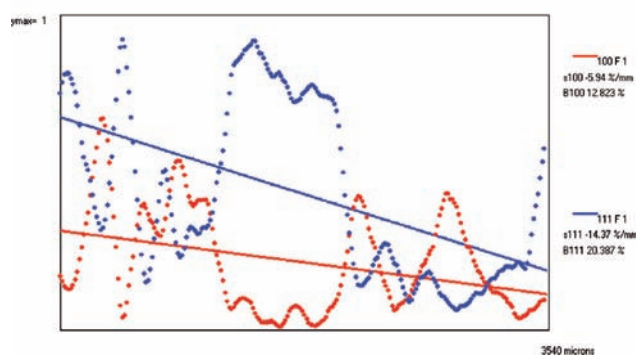


Figure 17: EBSD Grad plot of data set from figure 16 (straight line fit)

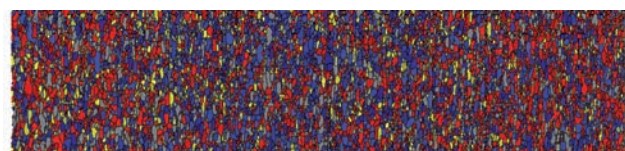


Figure 18: Plate with slight through-thickness gradient, and negligible banding (8 mm thick)

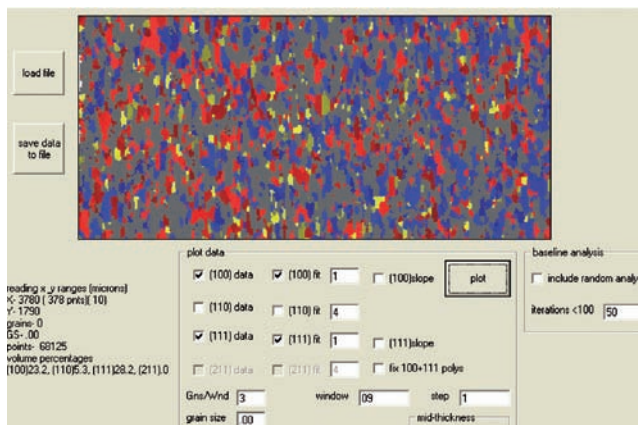


Figure 19: EBSD Grad working screen, left-half of figure 18

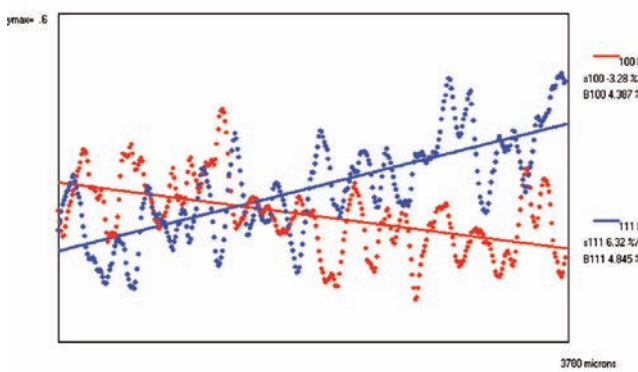


Figure 20: EBSD Grad plot of data set from figure 19 (straight line fit)

## UNIFORMITY ACROSS A PLATE, AND FROM PLATE TO PLATE

Above, non-uniformity within one sample (i.e. within an area which can easily be scanned by EBSD) has been considered. For process development work, many samples should be taken from as many plates as possible, and all the measurements (strength, gradient and banding severity of each component) can be used to compare sample to sample.

For quality control purposes (one sample may be taken per lot of plates, for example), the samples should be taken from equivalent locations. Control limits can be established for any (or all!) of the measurements and statistical control instituted. If a product is known to have some non-uniformity, which is accepted but must not vary except within established limits, a standard trend line (a polynomial) can be established for the product, and actual samples compared to that standard.

## COMPARISON TO ASTM E112 STANDARD FOR AVERAGE GRAIN SIZE

ASTM E112 describes methods for measuring and reporting average grain size. It is useable on many materials and on many product forms. It does not specify what the grain size should be, though, for any product. It is extremely useful to metallurgists everywhere. The proposal described above attempts to do the same thing for texture. It does not address only 'average' texture, though: it also addresses texture non-uniformities, which is why it has not proven possible to boil everything down to one measurement. Also, this proposed standard method for texture limits itself, at present, to plate. Possibly it could be expanded to cover other product forms.

## SUMMARY

An industry-wide group, specializing in tantalum sputtering targets, has formulated a method of quantifying texture, including degrees of non-uniformity, of plate, from standard EBSD data sets. The measurement parameters are, for each component of interest, (a) strength, (b) through-thickness gradient and (c) banding severity. These features are measured independently, which is important because banding, if present, is uncontrolled and varies from point to point and from plate to plate, whereas gradient is controlled by the manufacturing process. The measurement parameters correlate well with visual impressions of grain maps, and all evidence to date suggests that they correlate well with sputtering performance.

## REFERENCES

1. W.D. Westwood, Sputter Deposition, AVS, 2003
2. T. Nogami et al., Graded Ta/TaN/Ta Barrier for Copper Interconnects for High Electromigration Resistance, in Advanced Metallization Conference in 1998, MRS 1999, pp. 313 - 319
3. D. Fischer et al., Barrier and Contact Behaviour of Tantalum-based Thin Films for Use in Copper Metallization Scheme, *ibid*, pp. 337 - 344
4. C.A. Michaluk, D.B. Smathers and D.P. Field, Effect of Localized Texture on Sputter Performance of Tantalum, Proceedings of the Twelfth International Conference on Textures of Materials, NRC Research Press, Canada, 1999, pp. 1357 - 1362
5. Z. Zhang, L. Kho and C.E. Wickersham, Effect of grain orientation on tantalum magnetron sputtering yield. *Journal of Vacuum Science and Technology A*, 24(4), 2006, pp. 1107 - 1111
6. C.A. Michaluk, D.P. Field, K.A. Nibur, S.I. Wright and R.A. Witt, Effects of Local Texture and Grain Structure on the Sputtering Performance of Tantalum, *Materials Science Forum*, Vols 408-412, p.1615, 2002
7. R.S. Bailey and N.C. Hill, Effect of Sputtering Target Crystallographic Orientation on Step Coverage and Collimation Efficiency, *SPIE*, Vol 2637, 56 - 64, 2003
8. S. Turner, US Patent 6,331,233, issued 2001
9. P.R. Jepson et al, US Patent Application 10/079,286, Publication No. US 2002/0112789
10. C.A. Michaluk, M.M. Nowell and R.A. Witt, Quantifying the Recrystallization Texture of Tantalum, *JOM*, March 2002
11. Private Communications, J.A. Sutliff, 2004
12. A.J. Schwartz, M. Kumar, D.P. Field and B.L. Adams (eds), *Electron Backscatter Diffraction in Materials Science*, Kluwer Academic / Plenum Publishing, p. 34, 2000
13. R.S. Bailey, EBSDGrad, v.8, available from author

Please note our new office address:  
Tantalum-Niobium International Study Center,  
Chaussée de Louvain 490,  
1380 Lasne,  
Belgium.

## MEMBER COMPANY NEWS

### Herman Becker-Fluegel

The Tantalum-Niobium International Study Center was sad to learn that Herman Becker-Fluegel died in 2008 at the age of 80, and expresses sympathy to his family and colleagues.

Herman Becker-Fluegel was one of the founders of the T.I.C., working on the preparation to set up the organisation. He became one of the first members of the Executive Committee when the association was legally founded in 1974, with just three Committee members. He was the delegate of Tantalum Mining Company of Canada (Tanco) at that time, and later the delegate of National Resources Trading, another member company. He was also a director of numerous other mining and chemical companies across the world in his long career.

In September 1975 Mr Becker-Fluegel was elected as the second President of the T.I.C., by the Fourth General Assembly, serving as President until May 1977. It was in this capacity that he organised the first meeting to take place away from Brussels: the Seventh General Assembly, in the spring of 1977, was held in Winnipeg and included a mine visit to Tanco, initiating a tradition of plant and mine tours which continues to this day.

Mr Becker-Fluegel continued to serve on the Executive Committee until October 1985, and always remained a firm supporter of the T.I.C., taking a lively interest in its activities.

### Changes in member contact details

#### Anglo American Brasil

The nominated delegate to the T.I.C. for Anglo American Brasil is now Mr Jose Antonio de Lima.

E-mail: jose.lima@copebras.com.br (or contact Ms Fatima Cristina at fcristina@angloamerican.com.br).

#### Globe Metals & Mining Limited

Globe Metals & Mining Limited has relocated to the following address:  
Ground Floor, Suite 3, 16 Ord Street, West Perth WA6005, Western Australia.

The postal address, telephone and fax numbers remain the same:  
P.O. Box 1811, West Perth WA6872, Western Australia.

Tel.: +61-8-9486-1779, Fax: +61-8-9486-1718

#### Honeywell Belgium N.V.

Honeywell Belgium N.V. has nominated a new delegate to the T.I.C.: Mr Bjoern Jackisch, Global Business Manager Inorganic Fine Chemicals.

E-mail: bjoern.jackisch@honeywell.com

### Mamoré Mineração e Metalurgia Ltda/ Mineração Taboca S.A.

Mamoré Mineração e Metalurgia Ltda has been fully incorporated into Mineração Taboca S.A., therefore the company's membership is now in the name of Mineração Taboca S.A.

Ms Patricia Stumpf remains the nominated delegate to the T.I.C. Her new e-mail address is pstumpf@mtaboca.com.br.

### MTU Aero Engines GmbH

The nominated delegate to the T.I.C. for MTU Aero Engines GmbH is now Mr Wolfgang von Rützen-Kositzkau.

E-mail: Wolfgang.Ruetzen-Kositzkau@mtu.de

### NEC Tokin Corporation

Mr Masako Okeya has been nominated as new delegate to the T.I.C. for NEC Tokin Corporation.

E-mail: okeya@nec-tokin.com

### Simmonds (Metal Trading) Ltd

Simmonds (Metal Trading) Ltd has new telephone and fax numbers.

Tel.: +44-1485-517-045, Fax: +44-1485-517-046

## WORKING GROUP ON TANTALUM AND NIOBIUM MINING

The T.I.C. has established a Working Group on Tantalum and Niobium Mining. This Working Group is currently constituted of five members of the Executive Committee, together with the Technical Promotion Officer and the Secretary General. It held its first meeting in January 2009.

The objectives of the Working Group are to promote the tantalum and niobium industries, to explore the issues related to the mining of their minerals on a world-wide scale and to help to improve the standards of Artisanal and Small-scale Mining (ASM) operations. In particular, the Group is developing a policy of due diligence in the form of transparency and traceability of raw materials along the supply chain.

The timeline set out by the Working Group is the following: it aims to draft an outline proposal for discussion in April during the meeting of the Executive Committee, then to establish a policy to propose to the members of the association during the Fiftieth General Assembly in October, with a view to this policy taking effect by the end of 2009.